HOKKAIDO UNIVERSITY

Title	Active vibration control of automobile drivetrain with backlash considering time-varying long control period
Author(s)	Yonezawa, Heisei; Kajiwara, Itsuro; Nishidome, Chiaki; Hatano, Takashi; Sakata, Masato; Hiramatsu, Shigeki
Citation	Proceedings of The Institution of Mechanical Engineers Part D-journal of Automobile Engineering, 235(2-3), 773-783 https://doi.org/10.1177/0954407020949428
Issue Date	2021-02
Doc URL	http://hdl.handle.net/2115/80232
Rights(URL)	https://creativecommons.org/licenses/by-nc/4.0/
Type	article
File Information	0954407020949428.pdf

Instructions for use

Original Article

Active vibration control of automobile drivetrain with backlash considering time-varying long control period

Heisei Yonezawa[1], Itsuro Kajiwara[1] , Chiaki Nishidome[2], Takashi Hatano[3], Masato Sakata[3] and Shigeki Hiramatsu[3]

Abstract
Active vibration control of automotive drivetrains must be developed to compensate for the backlash of gears because it causes undesired responses. In addition, an engine used as an actuator has a constraint which makes the control periods longer and time-varying, resulting in deterioration of the control performance. The contribution of this study is to cope with all the issues described above, backlash and the control period constraint, simultaneously. First, a basic experimental device, which simplifies an actual vehicle to focus on the effect due to backlash, is demonstrated. In the device, the control period constraint, which is equivalent to that of an engine, is reproduced by a digital signal processor. To reduce an adverse effect due to the extension of the control period, the sampled-data controller, which does not require discretization in its implementation, is employed. In this paper, predictive processing using the servo-type sampled-data controller is proposed to compensate for the phase delay of the control input caused by the time-varying control period. In addition, a control mode switching technique included in the prediction suppresses undesired responses due to backlash. Finally, control experiments verify the effectiveness of the control system.

Introduction

Active damping of vibrations of automotive drivetrains remains a challenge to improve the riding comfort and driving performance of automobiles. In particular, when the engine torque changes suddenly (tip-in and tip-out), backlash of differential gears degrades the vibration control performance. Specifically, the shock torque, which is generated when the gear runs freely and collides in backlash, increases the vibration amplitude. To compensate for effects on controls due to backlash, example studies include the use of the descriptive function method,[1] the application of a neural network,[2] a fractional order proportional-integral-derivative (PID) controller,[3] a proposal for an adaptive fuzzy type H_∞ control,[4] the application of a H_∞ control,[5] and the modeling of backlash as a disturbance.[6] Regarding the control of automobile drivetrains with backlash, previous studies include an investigation of several nonlinear controllers based on PID control[7] and a proposal for a switching technique with linear-quadratic regulator (LQR) controllers.[8] In

particular, many outcomes are related to model predictive control (MPC).[9–14] These are broadly considered to be effective techniques. A mode-switching-based active control algorithm including the sliding mode technique and PID control has been investigated by simulation studies.[15]

In addition to the backlash problem, the limitations in the control period of actuators used for active damping of automotive drivetrains present additional problems. An example of such an actuator is the engine,[16] in which the generated torque corresponds to the control input. An engine cannot update the control input

[1]Division of Human Mechanical Systems and Design, Hokkaido University, Sapporo, Hokkaido, Japan
[2]CATEC Inc., Tokyo, Japan
[3]Mazda Motor Corporation, Hiroshima, Japan

Corresponding author:
Itsuro Kajiwara, Division of Human Mechanical Systems and Design, Hokkaido University, N13, W8, Kita-ku, Sapporo, Hokkaido, 060-8628, Japan.
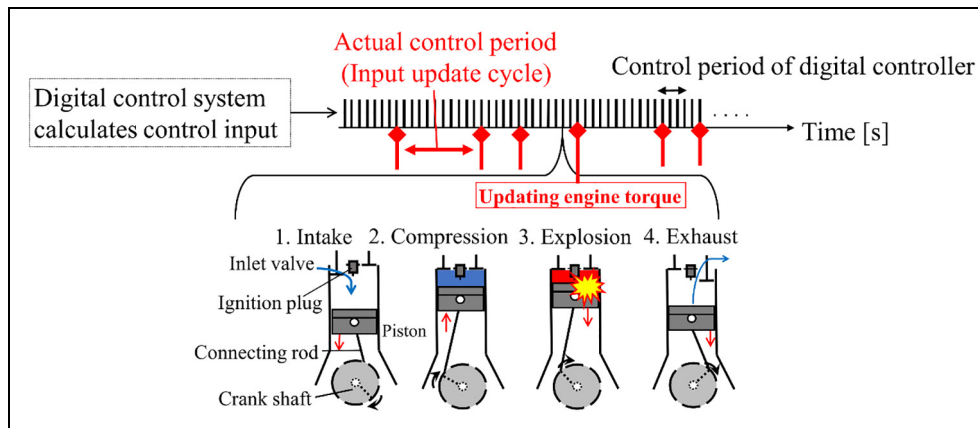Email: ikajiwara@eng.hokudai.ac.jp

Figure 1. Limitation of the control period due to the mechanism generating engine torque.

at the timing synchronized with that of a digital controller. This is due to the relationship shown in Figure 1 between the mechanism to update engine torque and the digital control cycles. An engine requires a series of processes (exhaust, intake, compression, explosion, and expansion) to update the generated torque value. In other words, the control input can only be updated at the moment when an explosion occurs in a combustion chamber and a crankshaft rotates by 180°. When an engine is used as an actuator, the intervals of the explosions, which depend on the engine speed, are the actual control periods. The two essential problems caused by this actuator constraint are

(A) Compared to the first resonant modes to be damped, the actual control periods are relatively long. Hence, a digital controller must be used (implemented) with the extended control periods, resulting in increased adverse effects of discrete approximation errors.
(B) The actual control periods are time-varying. This delays the phase of the control inputs, which can be generated by the actuator as command signals from a controller.

Although few studies have focused on the control period constraints with respect to active damping of automotive drivetrains, several notable studies have been proposed. The delay with the realization of a torque was modeled by the Pade approximation for controller design.[17] Modeling of an engine with a fixed maximal delay and the H_∞ controller design in continuous-time domain ensured the phase margin to cope with the mechanism to update engine torque.[18] In addition, predictive controllers have been proposed to compensate for the engine delay,[16,19,20] and their effectiveness has been experimentally validated.

In the previous works, however, it is not taken into account that the control periods of the actuator are made longer by problem (A), indicating that discrete approximation errors with traditional discretization are

not compensated for. In addition, the undesired response due to backlash, such as an overshoot, remains although it must be reduced. It means that compensation is not considered while backlash is traversed.

Compared to the previous studies, the present research addresses all the issues, the adverse effect due to backlash, and the control period constraints (A) and (B), simultaneously. The contribution of this study for active damping of automotive drivetrains is the combination of compensations for the following three issues:

(C1) Backlash causes the undesired response, such as an overshoot, under the condition where a driving force suddenly changes (tip-in and tip-out).
(C2) The control periods are relatively long compared to the period of the first resonant mode to be damped, corresponding to (A).
(C3) The control periods are variable depending on time, corresponding to (B).

In this study, a basic experimental device, which simplifies an actual vehicle to focus on the influence due to backlash while reproducing only the basic structure of the automotive drive system, is used to verify the control system.

In our previous study,[21] an approach to apply the sampled-data control to the extension of the control period (C2) was proposed. The sampled-data controller can explicitly consider responses between sample points because the design process does not require discrete approximations to implement. Hence, the controller implemented with a long control period prevents performance degradation due to discrete approximation errors even under the constraints. In the present paper, based on the previous study, a method for coping with the time-varying control periods (C3) is proposed. Because the time-varying control period causes phase delay of the control input actually updated by the actuator, predictive processing using the sampled-data controller is necessary. Specifically, a control input for

Table 1. Parameters of the experimental device.

Parameter	Value	Unit
M_B	0.232	kg
m_G	0.039	kg
M_E	1.04	kg
K_C	660.0	N/m
K_D	1.5×10^4	N/m
K_G	2.7×10^4	N/m
C_C	0.3	N s/m
C_D	7.5	N s/m
C_G	29.0	N s/m
C_{cl}	4.0	N s/m

the next step is predicted, and the predicted value is approximately used to compensate for the maximal phase delay for a command signal from the controller. In addition, a simple control mode switching algorithm to compensate for backlash is proposed, focusing on the adverse effects that occur when driving forces suddenly change. The compensation is performed while backlash is traversed, and it suppresses both the overshoot and the oscillations by reducing the shock of a collision. Finally, experiments using the basic experimental device verify effectiveness of the proposed control system.

Basic experimental device

Mechanical structure of the experimental device

The basic experimental device, which simplifies an actual vehicle to focus on the influence due to backlash while reproducing only the basic structure of the automotive drive system, is used as a controlled object. Figure 2(a) and (b) show the dynamical model and the real mechanism, respectively. Table 1 shows the device specifications. This is a three-degrees-of-freedom system, in which three weights (M_E, m_G, M_B) are connected by springs and dampers. Backlash is produced as a dead-zone band by creating a space between the leaf springs on both sides of the mass m_G. The more details on the experimental device such as the simplifications are included in Yonezawa and colleagues.[21,22]

Setting the control period constraint

The experimental device shown in Figure 2(b) uses a linear motor as an actuator. Because it is difficult to construct the real mechanism of an engine shown in Figure 1, only the control period constraint, which is equivalent to that of an engine, is given to the motor by a program in a digital signal processor (DSP). Figure 3(a) shows the conceptual closed-loop system of the control experiment. Even though the controller in the DSP can calculate the control inputs with short and constant periods, the program in the same DSP restricts the periods of actually updating the control inputs. It makes the actual control period longer and time-
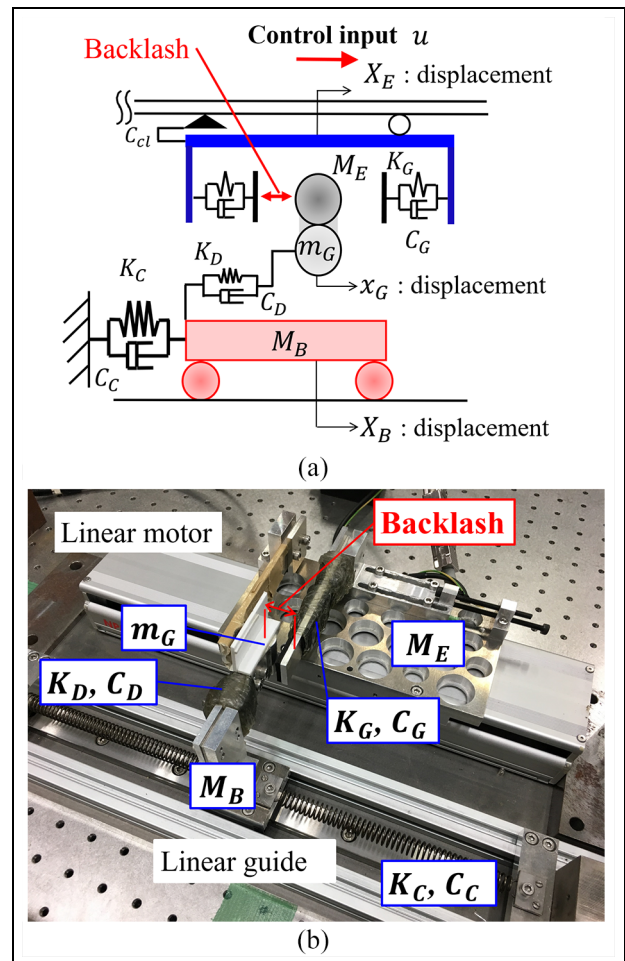

Figure 2. Basic experimental device: (a) dynamical model of the experimental device and (b) real mechanism.

varying. As a result, a thrust updated with the constrained periods drives the motor while the control input intended by the controller cannot be realized as is.

The actual (time-varying) control periods, as shown in Figure 3(b), are produced in the DSP as a constraint. The periods like that in Figure 3(b) were used and were approximately recorded in the control experiment demonstrated in the section "Control experiments." According to these control periods, the constraint program in the DSP holds the control input (motor thrust) to the same value, regardless of the new command from the controller. In Figure 3(b), the frequency to update the control input varies from approximately six to nine times the natural frequency (4 Hz) to be damped. Consequently, both the target conditions (C2) and (C3) are prepared.

Modeling

Since the experimental device has nonlinearities such as the backlash, the linearized model is necessary to design a sampled-data controller. The state equation and the output equation of the system are then derived as
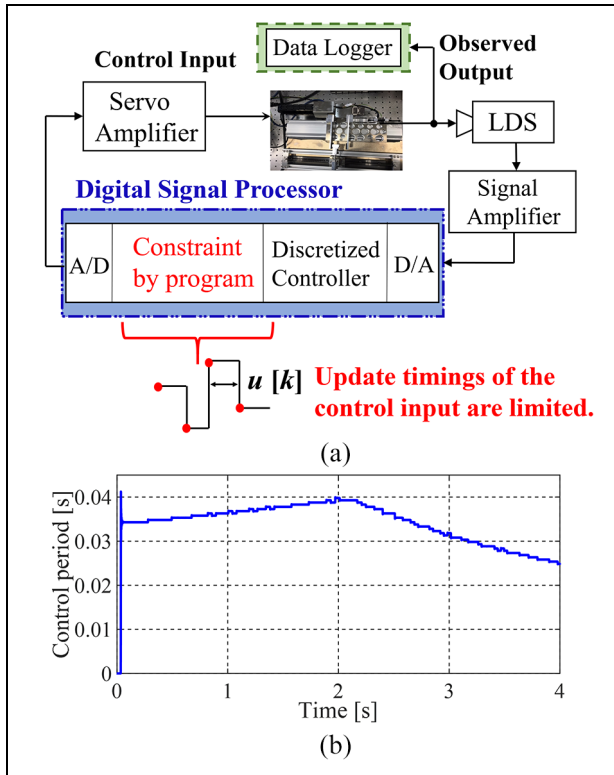
Figure 3. Experimental system using laser displacement sensor (LDS): (a) diagram of the closed-loop system and (b) time history of the control period, which is long and time-varying.

$$\dot{x}_p = A_p x_p + B_{p1} w_p + B_{p2} u \qquad (1)$$

$$y_p = C_p x_p + D_{p1} w_p + D_{p2} u \qquad (2)$$

Each coefficient matrix and the state variables are described as

$$
A_p =
\begin{bmatrix}
0 & 0 & 0 & 1 & 0 & 0 \\
0 & 0 & 0 & 0 & 1 & 0 \\
0 & 0 & 0 & 0 & 0 & 1 \\
-\dfrac{(K_D + K_C)}{M_B} & \dfrac{K_D}{M_B} & 0 & -\dfrac{(C_D + C_C)}{M_B} & \dfrac{C_D}{M_B} & 0 \\
\dfrac{K_D}{m_G} & -\dfrac{(SwK_G + K_D)}{m_G} & \dfrac{SwK_G}{m_G} & \dfrac{C_D}{m_G} & -\dfrac{(SwC_G + C_D)}{m_G} & \dfrac{SwC_G}{m_G} \\
0 & \dfrac{SwK_G}{M_E} & -\dfrac{SwK_G}{M_E} & 0 & \dfrac{SwC_G}{M_E} & -\dfrac{(SwC_G + C_{cl})}{M_E}
\end{bmatrix}
$$

$$
B_{p1} =
\begin{bmatrix}
0 & 0 \\
0 & 0 \\
0 & 0 \\
0 & \dfrac{1}{M_B} \\
\dfrac{1}{m_G} & 0 \\
-\dfrac{1}{M_E} & 0
\end{bmatrix},
B_{p2} =
\begin{bmatrix}
0 \\
0 \\
0 \\
0 \\
0 \\
\dfrac{1}{M_E}
\end{bmatrix},
C_p = \begin{bmatrix} 1 & 0 & 0 & 0 & 0 & 0 \end{bmatrix}
$$

$$D_{p1} = 0, D_{p2} = 0$$

$$\qquad (3)$$

$$x_p = \begin{bmatrix} X_B & x_G & X_E & \dot{X}_B & \dot{x}_G & \dot{X}_E \end{bmatrix}^T \qquad (4)$$

In equations (1) and (2), u is the motor thrust (control input), and w_p is the disturbance including force due to the backlash. Switching of the time-varying parameter Sw represents the dead-zone characteristic caused by backlash. The switching rule is written below.[23,24] $|\delta|$ is dead zone width and F is a force by the spring K_G. When designing the controller, the value of Sw is set as 1.0

$$F = Sw \cdot K_G \cdot \Delta X + OKG = Sw \cdot K_G \cdot (X_E - x_G) + OKG$$

$$
Sw =
\begin{cases}
1, & X_E - x_G > |\delta| \\
1, & X_E - x_G < -|\delta|, \\
0, & |X_E - x_G| \leqslant |\delta|
\end{cases}
$$

$$
OKG =
\begin{cases}
-|K_G \times |\delta||, & X_E - x_G > |\delta| \\
|K_G \times |\delta||, & X_E - x_G < -|\delta| \\
0, & |X_E - x_G| \leqslant |\delta|
\end{cases}
$$

$$\qquad (5)$$

The time-varying linear state equation of the experimental device with the backlash and other nonlinear characteristics is also described in Yonezawa et al.[22]

Compensation for extended control periods

According to the previous study,[21] the sampled-data H_2 controller[25–27] is applied to the plant to maintain the controller's performance even with the extended control period (C2). In the sampled-data control, involving no discrete approximations with the design allows responses between sampling points to be
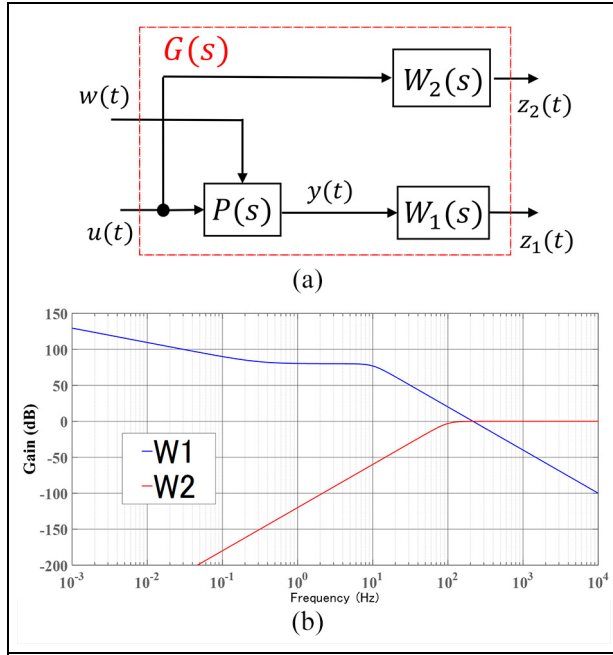
Figure 4. Design of the sampled-data controller: (a) generalized plant used to design the controller and (b) gain of the frequency weighting functions.

explicitly considered. Therefore, the implementation of the controller with a sampling period as long as possible prevents performance degradation due to the long intervals taken to update the control inputs. The designed controller is used in the predictive processing demonstrated in the next chapter.

Figure 4(a) shows a generalized plant used to design the controller. z_1 and z_2 are the controlled variables, and the displacement $y = X_B$ measured by the sensor is used as an observed output. The one example of the gain properties of each weighting function $W_j(s)$ ($j = 1, 2$) is shown in Figure 4(b) to demonstrate an effective control problem.

This study uses a weighting function $W_1(s)$ defined in the form of the following basic structure

$$M(s) = \frac{s + (2\pi \times \varepsilon_2)}{1.0} \quad (6)$$

$$\tilde{W}_1(s) = \frac{2.481 \times 10^5}{s^3 + 125.7s^2 + 7896s + 2.482 \times 10^5}$$
$$\times \frac{1.0}{s + (2\pi \times \varepsilon_1)} \quad (7)$$

$$W_1(s) = \tilde{W}_1(s) \cdot M(s) \quad (8)$$

The cut-off frequency ε_1 of the approximate integrator and the frequency ε_2 of the function $M(s)$ were designed as 10^{-10} and 0.3 Hz, respectively. When designing the controller, parameters of W_1 and W_2 need to be tuned to contribute to the good performance, which means a response satisfying both (P1) and (P2) shown below.

(P1) The transient vibration is sufficiently reduced.
(P2) The controlled variable follows the target signal with fewer steady errors.

The good control performance indicated above cannot be obtained by only tuning W_1 and W_2. Unless the sampled-data controller and the compensations presented later for the time-varying period and backlash are all used simultaneously, the best control performance that sufficiently achieves both (P1) and (P2) cannot be realized. One of them, the sampled-data controller (i.e. tuning of W_1 and W_2), partially contributes somewhat to the changes in the response.

The parameters of W_1 and W_2 were determined by actually conducting the experimental verifications while considering the qualitative relationship between each parameter and the above performance (P1) or (P2). Regarding the proposed control system, the tuning guideline based on the effects on (P1) and (P2) due to each parameter is presented below.

The low-pass filter in the first fraction of equation (7) is introduced to limit the controlled frequency band of the vehicle body vibration z_1 to a low-frequency band. For this reason, its cut-off frequency must be set as a low-frequency value that is not too high. Meanwhile, it must be set higher than the first natural frequency of the controlled object in consideration of the robustness against variations in the natural frequency. In this study, the cut-off frequency was determined as 10–30 Hz with a sufficient margin from the first natural frequency of 4.0 Hz. The gain in the passband of the low-pass filter becomes a weighting constant in minimizing the H_2 norm[25–27] of z_1 when designing the controller in Figure 4(a). Therefore, designing its value to be too small may lead to an insufficient transient vibration performance. For our experiments, the value of this gain was set as above 60 dB.

To reduce the steady errors with respect to the step target signal, it is necessary to make the approximate integrator $1/(s + (2\pi \times \varepsilon_1))$ in the second fraction of equation (7) an exact integrator $1/s$ as closely as possible. Consequently, ε_1 must be set as a sufficiently small positive value that is close to 0.

The multiplication of the approximate integrator in equation (7) by $M(s)$ in equation (6) can stop the gain of the approximate integrator from decreasing in the frequency band above ε_2. Accordingly, to prevent deterioration of the transient vibration due to decreases in the gain of the controlled frequency band (near the natural frequency) of $W_1(s)$, ε_2 must be designed such that "0 Hz $< \varepsilon_1 \ll \varepsilon_2 <$ natural frequency of the controlled object."

The high-pass filter $W_2(s)$ is employed to restrict the control input in a high-frequency band. Therefore, its cut-off frequency must be sufficiently higher than the passband (i.e. controlled frequency band) of the above low-pass filter. In addition, because the gain of W_2 becomes a weighting constant in restricting the control
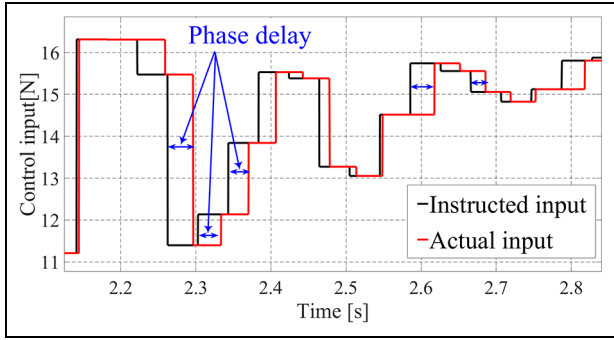
Figure 5. Phase difference between instructed inputs from the controller and inputs actually updated by the actuator.

input z_2 in Figure 4(a), it should be tuned to be smaller than that of W_1, especially when the transient vibration needs to be improved.

Compensation for time-varying control periods

Phase delay of the control input

Figure 5 shows the control simulation result. This is an enlarged graph of the control inputs where a sampled-data controller with a fixed control period is directly applied to the plant, which has a time-varying control period. The black and red lines indicate the command signal from the controller (hereafter the instructed input) and the control input actually driving the actuator (hereafter the actual input), respectively.

The effect due to the time-varying control period (C3) appears in the form of a phase delay in the control input. As seen from Figure 5, the phase difference between the instructed and actual inputs is an adverse effect to control systems. The phase of the actual input (red line) is always delayed. In the second half of the control period, an actual input is updated as the instructed input of nearly one whole past step. This produces the most adverse effect on control systems.

One step ahead prediction with backlash compensation

In this study, predictive processing for one step ahead compensates for the delay. This compensates for the most adverse case, where an actual input is updated in the second half of the control period. To improve the control performance, an actual input should follow the instructed input calculated at the step nearest to the actual update time. Consequently, in the second half of the control period, the predicted input one step ahead is approximately used as the instruction.

Here, a conceptual scheme of the proposed control system is described. Figure 6 outlines the compensation method, assuming that the current time is $t = n\Delta T_s$. ΔT_{cont}, ΔT_s, and $\Delta T_{predict}(\geqslant \Delta T_s)$ are a constant period of the sampled-data controller, a calculation interval in the DSP, and a simulation period for the predictive calculation, respectively. k, n, and i represent the number of steps with respect to ΔT_{cont}, ΔT_s, and $\Delta T_{predict}$, respectively. In Figure 6, when the actuator cannot update the actual input, even in the second half of ΔT_{cont}, the predictive calculation with the interval of $\Delta T_{predict}$ approximately obtains the control input $u(k + 1)$ at $(k + 1)\Delta T_{cont}$ of the next step.

Specifically, a simulation of the plant from $t = n\Delta T_s$ to $t = (k + 1)\Delta T_{cont}$ consisting of total N_{pre} steps is performed as

$$
\begin{aligned}
\boldsymbol{x}_{pd}[i + 1] &= \boldsymbol{A}_{pd}\boldsymbol{x}_{pd}[i] + \boldsymbol{B}_{p1d}\boldsymbol{w}_p[i] + \boldsymbol{B}_{p2d}u[i] \\
&= \{\boldsymbol{I} + \Delta T_{predict} \cdot \boldsymbol{A}_p(t)\}\boldsymbol{x}_{pd}[i] \\
&\quad + \{\Delta T_{predict} \cdot \boldsymbol{B}_{p1}(t)\}\boldsymbol{w}_p[i] + \{\Delta T_{predict} \cdot \boldsymbol{B}_{p2}(t)\}u[i]
\end{aligned}
$$

(9)

$$
y_{pd}[i] = \boldsymbol{C}_{pd}\boldsymbol{x}_{pd}[i] + \boldsymbol{D}_{p1d}\boldsymbol{w}_p[i] + D_{p2d}u[i] = \boldsymbol{C}_p(t)\boldsymbol{x}_{pd}[i]
$$

(10)

where

$$
i = 0, 1, 2, \ldots, N_{pre}
$$

(11)

$$
N_{pre} = \frac{(k + 1)\Delta T_{cont} - n\Delta T_s}{\Delta T_{predict}} + 1
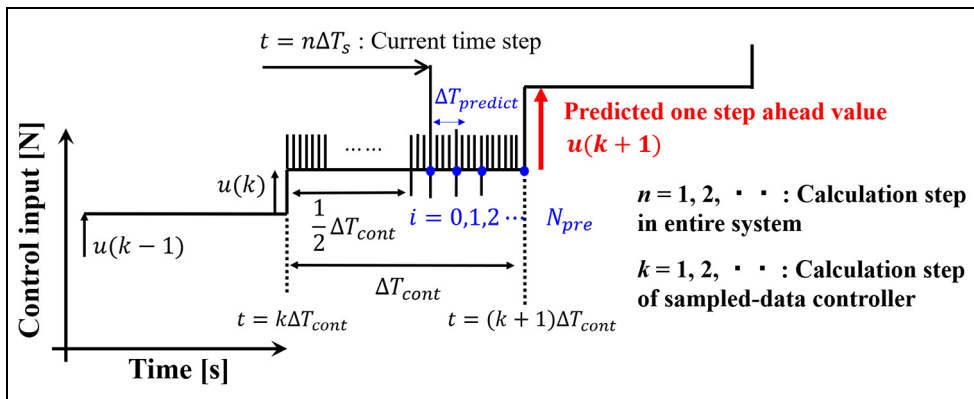$$

(12)

Figure 6. Conceptual scheme of one step ahead prediction to compensate for the phase delay.

Using the time-varying linear state equation of the experimental device with nonlinearities such as the backlash,[22] each coefficient matrix in equations (9) and (10) is obtained online. It is also used for the state estimation demonstrated later. In equations (9) and (10), $u[i]$ is the control input driving the actuator, and $w_p[i]$ is the external input including the term due to backlash. The discrete-time coefficient matrices in equations (9) and (10) are approximately obtained from the continuous-time model.

The simulation requires initial conditions, which correspond to the state quantities $x_{pd}[i]$ of the plant. Based on the Kalman filtering theory using the time-varying linear state equation, they are estimated as equations (13)–(17). Here, Q and R are covariance matrices of system noise and observation noise, respectively. The covariance matrices Q and R are given by multiplications of each unit matrix by scalar gains "q" and "r," respectively.

This study attaches relatively more importance to robustness against uncertainties of the real device than compensation for accuracy of the sensor. Therefore, the covariance matrices were tuned to be a relatively large "q" and a small "r." With respect to the vibration during the mechanical contact occurring in the backlash, this tuning policy is aimed at making the contribution of the observed output to the estimation result larger than that of the estimation process equations (13) and (14) using only the plant model in the Kalman filter. In addition, Q and R were determined by actually conducting experimental verifications in which the state variables were estimated.

(Step 1). A priori estimate

$$\hat{x}_{pd}^-[n] = A_{pd}[n-1]\hat{x}_{pd}[n-1]$$
$$+ B_{p1d}[n-1]w_p[n-1] + B_{p2d}[n-1]u[n-1]$$
$$= \{I + \Delta T_s A_p((n-1)\Delta T_s)\}\hat{x}_{pd}[n-1]$$
$$+ \Delta T_s[\, B_{p1}((n-1)\Delta T_s) \quad B_{p2}((n-1)\Delta T_s)\,]$$
$$\begin{bmatrix} w_p[n-1] \\ u[n-1] \end{bmatrix}$$

(13)

(Step 2). A priori covariance matrix

$$P^-[n] = A_{pd}[n-1]P[n-1]A_{pd}^T[n-1]$$
$$+ [\, B_{p1d}[n-1] \quad B_{p2d}[n-1]\,]Q\begin{bmatrix} B_{p1d}^T[n-1] \\ B_{p2d}^T[n-1] \end{bmatrix}$$
$$= \{I + \Delta T_s A_p((n-1)\Delta T_s)\}P[n-1]\{I + \Delta T_s A_p((n-1)\Delta T_s)\}^T$$
$$+ (\Delta T_s)^2[\, B_{p1}((n-1)\Delta T_s) \quad B_{p2}((n-1)\Delta T_s)\,]Q\begin{bmatrix} B_{p1}^T((n-1)\Delta T_s) \\ B_{p2}^T((n-1)\Delta T_s) \end{bmatrix}$$

(14)

(Step 3). Kalman gain

$$g[n] = P^-[n]C_p^T(n\Delta T_s)\left(C_p(n\Delta T_s)P^-[n]C_p^T(n\Delta T_s) + R\right)^{-1}$$

(15)

(Step 4). An estimated state quantity

$$\hat{x}_{pd}[n] = \hat{x}_{pd}^-[n] + g[n]\{y_{pd}[n] - C_p(n\Delta T_s)\hat{x}_{pd}^-[n]\}$$

(16)

(Step 5). A posteriori covariance matrix

$$P[n] = \{I - g[n]C_p(n\Delta T_s)\}P^-[n]$$

(17)

Specifically, q and r were determined as 5.0×10^9 and 5.0×10^0, respectively.

Compensation for backlash:

To predict the control input at $t = (k+1)\Delta T_{cont}$, the sampled-data controller (A_c, B_c, C_c, D_c) is performed. In this study, the adverse effect due to backlash is addressed under the condition where a target signal $r(t)$ suddenly changes stepwise (tip-in and tip-out). The compensation prevents accumulation of the control errors in backlash and allows it to be traversed quickly but smoothly. Considering the characteristic of real vehicles, this is performed during a minute dead time, which is also set for the experimental device before the change of the target signal.[22] Specifically, the control mode switching shown in Figure 7 is applied to the sampled-data controller.

Control Mode I is the normal control that operates during the mechanical contact in backlash. Control Mode II performs the compensation while backlash is traversed. Here, switching the target signal to a small positive value r_{pre} reduces backlash gently, and anti-windup, which temporarily stops updating the state variable $x_c(k)$ in the controller, avoids accumulation of the control errors. As a result of this compensation, unnecessary large control inputs are prevented, leading to a greatly reduced shock force with a collision in backlash. Two kinds of the values r_{pre} need to be prepared and tuned. One is the threshold value to switch the target signal, and another is used to calculate the errors. See Yonezawa et al.[22] for more details on the backlash compensation. In this study, it is modified so as to be combined with the predictive processing. When the control mode at $k\Delta T_{cont}$ is any other than Control Mode I, the backlash compensation shown in Figure 7 is used in the prediction.

Control Mode I:

$$x_c(k+2) = A_c x_c(k+1) + B_c\left(y_{pd}[N_{pre}] - r(n\Delta T_s)\right)$$

(18)

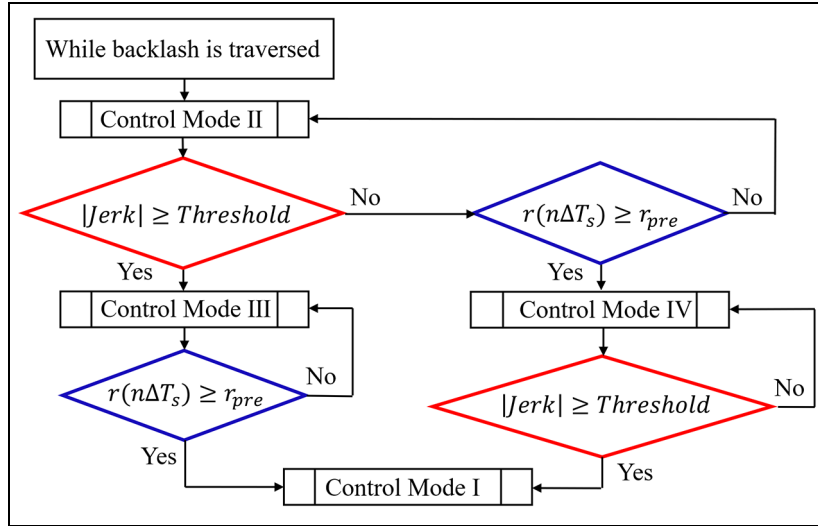**Figure 7.** Flow chart of switching control modes.

$$u(k + 1) = C_c x_c(k + 1)$$
$$+ D_c(y_{pd}[N_{pre}] - r(n\Delta T_s)) + K_C r(n\Delta T_s)$$
$$(19)$$

Control Mode II:

$$x_c(k + 2) = A_c\{z^{-1}[x_c(k + 1)]\} + B_c(y_{pd}[N_{pre}] - r_{pre})$$
$$(20)$$

$$u(k + 1) = C_c\{z^{-1}[x_c(k + 1)]\}$$
$$+ D_c(y_{pd}[N_{pre}] - r_{pre}) + K_C r_{pre} \quad (21)$$

Control Mode III:

$$x_c(k + 2) = A_c x_c(k + 1) + B_c(y_{pd}[N_{pre}] - r_{pre})$$
$$(22)$$

$$u(k + 1) = C_c x_c(k + 1)$$
$$+ D_c(y_{pd}[N_{pre}] - r_{pre}) + K_C r_{pre} \quad (23)$$

Control Mode IV:

$$x_c(k + 2) = A_c\{z^{-1}[x_c(k + 1)]\}$$
$$+ B_c(y_{pd}[N_{pre}] - r(n\Delta T_s)) \quad (24)$$

$$u(k + 1) = C_c\{z^{-1}[x_c(k + 1)]\}$$
$$+ D_c(y_{pd}[N_{pre}] - r(n\Delta T_s)) + K_C r(n\Delta T_s)$$
$$(25)$$

Figure 7 indicates the conditions to switch each control mode. In particular, to identify mechanical contact in backlash, a jerk, which is obtained by differentiating the acceleration of the vehicle body with respect to time, is used as the threshold condition.

Control experiments

Verification of fixed long control period

First, a sampled-data controller is verified for the plant with the fixed control period constraint (only (C2)).[21] The long control period of (C2) is determined as

$\Delta T_{cont} = 0.0404$ s. For comparison, a traditional continuous-time H_2 controller implemented by discretization is also applied. In addition, the experimental results for a sufficiently short control period ($\Delta T_{cont} = 0.005$ s) are presented to clearly indicate the effect on the period extension.

Figure 8 shows the experimental results under the constraint of the fixed control period (only (C2)). The upper and lower graphs show the time history waveforms of the vehicle body vibration and the control input, respectively. The blue line is the response without control and the green line is the target signal to be followed. The red and black lines indicate the results obtained by a sampled-data controller and a continuous-time controller, respectively. Specifically, the solid lines mean that controllers are verified for the long control period (Legend: "Sd-H2 long" and "C-H2 long"), while the results for the short period are shown in the dotted lines (Legend: "Sd-H2 short" and "C-H2 short").

Verification of time-varying long control period

Next, the experimental results under the condition where the control period is long (C2) and time-varying (C3) are presented. Regarding the proposed control system, ΔT_s, ΔT_{cont}, and $\Delta T_{predict}$ were determined to be 0.5×10^{-3}, 0.0404, and 0.5×10^{-3} s, respectively. In particular, ΔT_{cont} of a sampled-data controller was determined to be exceeding the longest value in the range of the time-varying control periods.

Figure 9 shows the experimental results under the constraints (C2) and (C3). As one of the worst cases, the magenta line indicates the response without compensation (predictive processing) for the time-varying period. The yellow line shows the result without compensation for backlash, although the control period constraints (C2) and (C3) are dealt with. The red line indicates the control result from the proposed method,
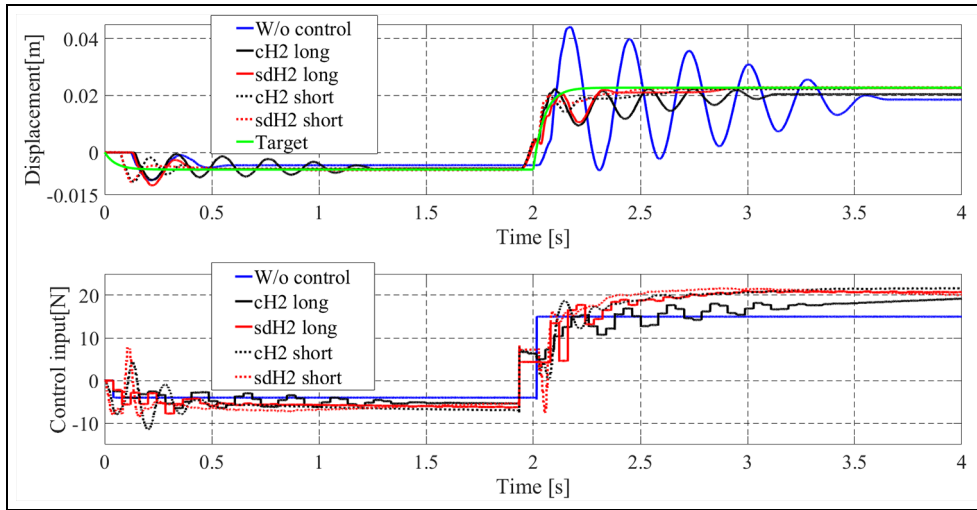
Figure 8. Displacement and control input obtained by the control experiments when the control period is fixed.
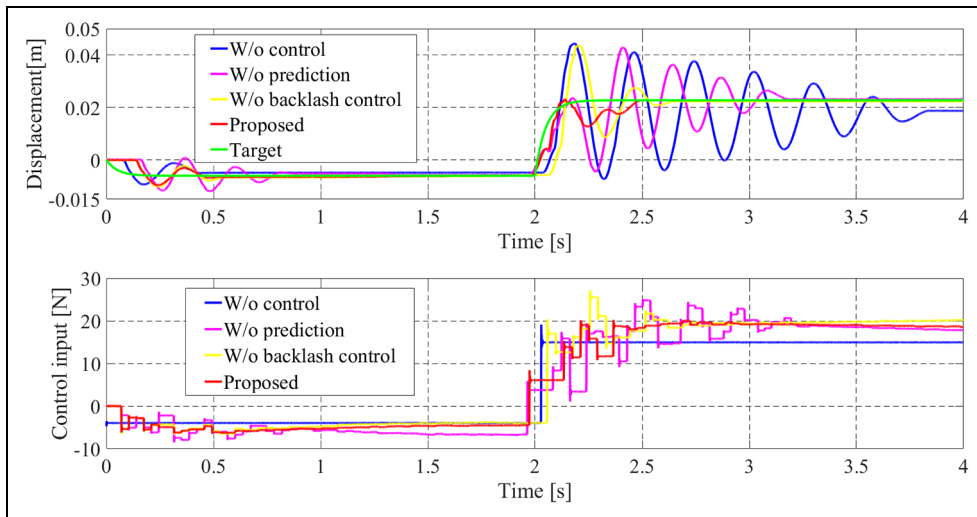

Figure 9. Displacement and control input obtained by the control experiments when the control period is time-varying.

which simultaneously compensates for all the control period constraints (C2) and (C3), and backlash.
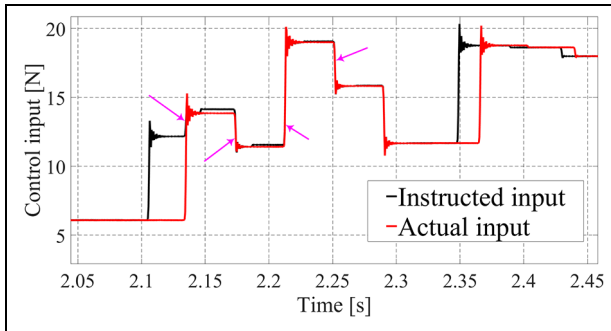
Discussion

Figure 8 demonstrates the improvement by the sampled-data controller for the control period constraint (C2). Both the sampled-data H_2 controller and the continuous-time H_2 controller perform the good performances with sufficiently short control period. However, the continuous-time controller deteriorates in performance with the long control period due to the effect of discrete approximation errors. On the other hand, the sampled-data controller maintains the high damping performance even under the constraint. Table 2 expresses the performance obtained by each control system as quantitative evaluation indices. It also demonstrates the above effectiveness of the sampled-data controller against the long control period. "None" in Table 2 means that the overshoot with respect to the

steady value of the target signal did not occur. The settling time is the time that the output takes to achieve and remain within a specified error range ±5% around the steady value of the target signal. Regarding the control system that could not settle the output within the range, it is expressed as "Unconverged" in Table 2. More detailed considerations on the performance differences between the two controllers can be found in the literature.[21]

For the constraints (C2) and (C3), Figure 9 shows good control performance, demonstrating the effectiveness of the proposed approach described in the section "Compensation for time-varying control periods." Specifically, the transient vibration that occurs after backlash is traversed (after 2 s) is greatly reduced with the compensation for the time-varying period (the red line) compared to that without compensation (the magenta line). This improvement indicates that the predicted input for the next step is appropriate to compensate for the phase delay. Figure 10 is an enlarged graph

Table 2. Comparison of the control performances with the fixed control period using quantitative evaluation indexes.

Control results	Overshoot (m)	Settling time (s)
Without control	0.0214 (Peak time: 2.173 s)	Unconverged
C-H2 long	None	Unconverged
Sd-H2 long	None	2.847
C-H2 short	None	2.6514
Sd-H2 short	None	2.451

Table 3. Comparison of the control performances with the time-varying control period using quantitative evaluation indexes.

Control results	Overshoot (m)	Settling time (s)
Without control	0.0217(Peak time : 2.1836s)	Unconverged
Without prediction	0.0201(Peak time : 2.411s)	3.152
Without backlash control	0.0207(Peak time : 2.198s)	2.617
Proposed	0.00033(Peak time : 2.138s)	2.465

Figure 10. Enlarged graph of the control inputs obtained from the proposed control system.

of the control inputs obtained from the proposed method. The variation in switching interval of the instructed input and the elimination of the phase delay suggest that the predicted inputs can be given as instructions, as shown by the arrows. These phase compensations immediately after backlash is traversed contribute to the vibration improvement. However, only the predictive processing may have difficulty in ensuring robustness of the damping performance because the compensation for the update timing at near $(k + 1/2)\Delta T_{cont}$ is insufficient. Hence, the enhancement of the present approach is included in our future tasks.

Next, the improvement thanks to backlash compensation is evaluated from a comparison between the red and yellow lines in Figure 9. Without the control mode switching (the yellow line), overshooting occurs just after the target signal rises due to backlash. When the target signal suddenly changes at 2 s, because an uncontrollable time zone due to backlash causes control errors to accumulate, the controller calculates unnecessarily large control inputs, resulting in a collision and a large shock force. On the other hand, with the compensation for backlash (the red line), a high control performance to suppress the overshooting is obtained. From the control input, it is demonstrated that backlash is reduced beforehand during the dead time. Furthermore, the anti-windup prevents excessive control inputs, and backlash is gently traversed.

The above control performances shown in Figure 9 are also summarized in Table 3 as the quantitative evaluation indices. Table 3 quantitatively confirms the effectiveness of the proposed control system, which

consists all of the sample-data controller, the predictive processing for the time-varying effect, and the backlash compensation.

Regarding W_1 and W_2, incorrect tuning, which clearly violates the design guideline presented in the "Compensation for extended control periods" section, will degrade the control performance. For example, if the cut-off frequency of the low-pass filter is set below the natural frequency, the transient vibration may deteriorate because the vibration component that should be suppressed is not effectively reflected in z_1 in Figure 4(a) due to its stopband. Too large ε_1 may increase steady errors by weakening the effect of the approximate integrator. However, as long as each parameter is within the range of its correct values presented in the "Compensation for extended control periods" section, the control performance may be robustly ensured even if its value roughly varies. This is because all values within the correct range satisfy the intent of each parameter toward the performance (P1) or (P2).

While the plant model used for the Kalman filter has some uncertainties such as frictional characteristics, it can mostly reproduce the macro behavior of the experimental device such as the low-frequency vibration that should be controlled. Therefore, even if the covariance matrices are tuned to be a small "q" and a large "r," the control performance may not remarkably deteriorate.

Conclusion

This study proposed an active vibration control method for automotive drivetrains with backlash considering the constraint on control periods. First, the basic experimental device, which simplifies an actual vehicle to focus on the backlash while reproducing only the basic phenomena of the drivetrain, was described. In experiments, a motor with the control period constraint, which is equivalent to that of an engine, makes control periods longer and time-varying. To compensate for the constraint, predictive processing using the servo-type sampled-data controller was presented. Furthermore, the control mode switching technique included in the prediction suppressed the undesired responses due to backlash. Finally, the proposed approach was verified experimentally, demonstrating its high control performance.

In the future, the practicality of the proposed method needs to be verified by applying it to real vehicle drivetrains. In addition, we will investigate the sensitivity of the control performance to the tuning of the control system parameters in more detail. Furthermore, studies on the enhancement of robustness of the control system against various verification conditions and controller tuning, which are more quantitative and theoretical, are also necessary.

Declaration of conflicting interests

The author(s) declared no potential conflicts of interest with respect to the research, authorship, and/or publication of this article.

Funding

ORCID iD

Itsuro Kajiwara ⓘD https://orcid.org/0000-0003-2651-7289

References

1. Dhaouadi R, Kudo K and Tobise M. Analysis and compensation of speed drive systems with torsional loads. *IEEE T Ind Appl* 1994; 30: 760–766.
2. Seidl DR, Lam SL, Putman JA, et al. Neural network compensation of gear backlash hysteresis in position-controlled mechanisms. *IEEE T Ind Appl* 1995; 31: 1475–1483.
3. Barbosa RS and Tenreiro Machado JA. Limit cycle prediction of systems with fractional controllers and backlash. *J Vib Control* 2017; 23: 587–603.
4. Wu TS, Karkoub M, Wang H, et al. Robust tracking control of MIMO underactuated nonlinear systems with dead-zone band and delayed uncertainty using an adaptive fuzzy control. *IEEE T Fuzzy Syst* 2017; 25: 905–918.
5. Ponce IU, Orlov Y, Aguilar LT, et al. Nonsmooth H∞ synthesis of non-minimum-phase servo-systems with backlash. *Control Eng Pract* 2016; 46: 77–84.
6. Acho L, Ikhouane F and Pujo G. Robust control design for mechanisms with backlash. *J Control Eng Techn* 2013; 3: 175–180.
7. Lagerberg A and Egardt B. Evaluation of control strategies for automotive powertrains with backlash. In: *6th international symposium on advanced vehicle control*, Hiroshima, Japan, 9–13 September 2002, pp.517–522. Göteborg: Chalmers Reproservice.
8. Templin P and Egardt B. A powertrain LQR-torque compensator with backlash handling. *Oil Gas Sci Technol* 2011; 66: 645–654.
9. Lagerberg A and Egardt B. Model predictive control of automotive powertrains with backlash. *IFAC P Vol 2005*; 38: 1–6.
10. Caruntu CF, Balau AE, Lazar M, et al. Driveline oscillations damping: a tractable predictive control solution based on a piecewise affine model. Nonlinear Anal: Hybri 2016; 19: 168–185.
11. Formentini A, Oliveri A, Marchesoni M, et al. A switched predictive controller for an electrical powertrain system with backlash. *IEEE T Power Electr* 2017; 32: 4036–4047.
12. Atabay O, Ötkür M and Ereke İM. Model based predictive engine torque control for improved drivability. *Proc IMechE, Part D: J Automobile Engineering* 2018; 232: 1654–1666.
13. Rostalski P, Besselmann T, Barić M, et al. A hybrid approach to modeling, control and state estimation of mechanical systems with backlash. *Int J Control* 2007; 80: 1729–1740.
14. Lu X, Lu T and Chai B. Mode-switch model predictive controller with "pre-contact" method for alleviating driveline vibration of electric vehicles considering backlash. *Proc IMechE, Part D: J Automobile Engineering* 2020; 234: 2176–2194.
15. Lv C, Zhang J, Li Y, et al. Mode-switching-based active control of a powertrain system with non-linear backlash and flexibility for an electric vehicle during regenerative deceleration. *Proc IMechE, Part D: J Automobile Engineering* 2015; 229: 1429–1442.
16. Berriri M, Chevrel P and Lefebvre D. Active damping of automotive powertrain oscillations by a partial torque compensator. *Control Eng Pract* 2008; 16: 874–883.
17. Richard S, Chevrel P and Maillard B. Active control of future vehicles drivelines. In: *Proceedings of the 38th IEEE conference on decision and control*, Phoenix, AZ, 7–10 December 1999, pp.3752–3757. New York: IEEE.
18. Lefebvre D, Chevrel P and Richard S. An H-infinity-based control design methodology dedicated to the active control of vehicle longitudinal oscillations. *IEEE T Contr Syst T* 2003; 11: 948–956.
19. Baumann J, Torkzadeh DD, Ramstein A, et al. Model-based predictive anti-jerk control. *Control Eng Pract* 2006; 14: 259–266.
20. Berriri M, Chevrel P and Lefebvre D. Varying sampling predictive control for time delay systems: application to automotive powertrain control. *IFAC P Vol 2007*; 40: 89–96.
21. Yonezawa H, Kajiwara I, Nishidome C, et al. Vibration control of automotive drive system with backlash considering control period constraint. *J Adv Mech Des Syst* 2019; 13: 1800430.
22. Yonezawa H, Kajiwara I, Sato S, et al. Vibration control of automotive drive system with nonlinear gear backlash. *J Dyn Syst* 2019; 141: 121002.
23. Gerdes JC and Kumar V. An impact model of mechanical backlash for control system analysis. In: *Proceedings of 1995 American control conference—ACC'95*, Seattle, WA, 21–23 June 1995, pp.3311–3315. New York: IEEE.
24. Nordin M, Galic J and Gutman P-O. New models for backlash and gear play. *Int J Adapt Control* 1997; 11: 49–63.
25. Chen TC and Francis BA. H2-optimal sampled-data control. *IEEE T Automat Contr* 1991; 36: 387–397.
26. Khargonekar PP and Sivashankar N. H2 optimal control for sampled-data systems. *Syst Control Lett* 1991; 17: 425–436.
27. Bamieh B and Pearson JB. The H2 problem for sampled-data systems. *Syst Control Lett* 1992; 19: 1–12.